

Influence of beam speed on residual stresses in the vicinity of laser welds

ANEV Nikolaj^{1, a}, KOLAŘÍK Kamil^{2, b}, PALA Zdenek^{3, c *},
NĚMEČEK Stanislav^{4, d}, ČAPEK Jiří^{5, e}

^{1,2,3,5}Faculty of Nuclear Sciences and Physical Engineering, Czech Technical University in Prague,
Trojanova 13, 12000 Prague, Czech Republic

⁴MATEX PM, Morseova 5, 301 00 Pilsen, Czech Republic

^anikolaj.ganev@fjfi.cvut.cz, ^bkamil.kolarik@fjfi.cvut.cz, ^czdenek.pala@fjfi.cvut.cz,
^dnemecek@matexpm.com, ^ecapekjir@fjfi.cvut.cz

Keywords: laser welding, high-power diode laser, X-ray diffraction, beam speed

Abstract. One of the drawbacks of the laser welding is distortion of the welded bodies that is closely linked with the generation and redistribution of residual stresses in the vicinity of the weld. In this contribution, mapping of surface macroscopic residual stresses and grain sizes was performed for several welds created with the laser beam with various speeds. Larger distortions are exhibited by samples manufactured with higher laser beam speed, which also exhibit substantial compressive residual stresses perpendicularly to the welds axis.

Introduction

Analysis of residual stresses in welds embodies an important industrial application of both X-ray and neutron diffraction for several decades. Neutron diffraction is employed when coarser grains are present in the analysed area of the material and when non-destructive spatial distribution of residual stresses is of interest. On the other hand, precise mapping of residual stresses in the surface layer not deeper than 10 microns calls for X-ray diffraction. Results obtained by these techniques serve not only as quality control, but the vital parameters of welding are being tuned according to joint evaluation of welds' microstructure and residual stress field in the vicinity of the welds. Unfavourable residual stresses can lead to shortening of service life, especially when the welds are parts of dynamically loaded components, such as in a commonplace in weld produced in automotive, aeronautics or power industries. All these industries cherish not only good reproducibility and high degree of automation of the welding process, but also contactless character and reliability of the used apparatus. Laser welding with high-power diode laser (HPDL) belongs to welding techniques that fulfil all the above mentioned requirements and the obtained welds comply with very stringent demands for small heat-affected zone, fewer cracks and lower porosity or, in general, compact microstructure [1]. Apart from these virtues, there is one nuisance that lies in the character of the HPDL beam which is divergent. When tiny objects are to be joined together, it can be fairly problematic to obtain suitably small laser beam.

Ill-calculated and ill-tuned laser welding process could lead to unfavourable microstructure with pores and oxides which can only be aggravated by tensile residual stresses and in the effect form close-to-ideal conditions for crack propagation and ultimately, object failure. The aim of the laser welding process is, thus, not only to produce a joint, but also to (i) avoid generation of tensile residual stresses and to (ii) minimize the distortion of the final object. It has been found [2] that distortion and the macroscopic residual stresses after welding are two mutually affected phenomena and, therefore, upon controlling the residual stresses by the means of laser beam energy and speed of the weld creation, one can influence the undesirable distortion as well.

In this contribution, mapping of surface macroscopic residual stresses in two directions, i.e. parallel and perpendicular to the welds axis, were performed for two bodies. The first contained

a weld created with a HPDL beam speed of 2 m/min and the second with a much more cost-effective speed of 15 m/min. Our aim was to compare not only resulting fields of residual stresses, but also to perform qualitative assessment of the possible presence of crystallographic texture and gain a qualitative apprehension about the grain sizes in the vicinity of a laser weld joining two steel sheets. Moreover, diffraction line broadening as a parameter of the degree of plastic deformation was evaluated from the measured profiles.

Experimental

The analysed bodies were manufactured by welding of two sheets made from S355 steel. Power of the HPDL was set to 3.5kW; the speed of welding was 2 m/min and 15 m/min. The lengths of the welds were approximately 180 mm. The thickness of the steel sheets was chosen correspondingly to both the chosen velocities of laser beam and the necessity to obtain a proper weld.

Angular distortions of both bodies were measured in six equidistant points in the direction perpendicular to the welds; the obtained values were, thus, 6 angles of deflection.

The structure of the welds and the adjacent areas of the steel sheets were qualitatively characterized by 2D diffraction patterns, or more precisely by Debye rings of $\{211\}$ planes of α -Fe obtained in the backscattering layout of Debye-Scherrer method. For this purpose, ISO DEBYEFLEX 3003 apparatus, non-filtered radiation from X-ray tube with chromium anode, cylindrical primary collimator 1 mm in diameter and image plate detector were employed.

Surface distributions of macroscopic residual stresses were measured perpendicularly to the welds in eleven areas mutually shifted by 0.5 mm. Each analysed area had a rectangular shape with dimensions $10 \times 0.5 \text{ mm}^2$; the longer sides being parallel with the welds. Stresses determined in the directions parallel with the welds are termed longitudinal stresses σ_L , and perpendicular transverse stresses σ_T .

We assumed biaxial state of stress and used the „ $\sin^2\psi$ “ [3] method coupled with Winholtz-Cohen least squares fitting procedure [4] to compute both the longitudinal and transverse stresses. The measured diffraction profile of α -Fe $\{211\}$ planes has for the used filtered $\text{CrK}\alpha$ radiation its maximum at $2\theta \approx 156^\circ$. Detected doublets were separated by Rachinger method [5] to the contributions from $\text{CrK}\alpha_1$ and $\text{CrK}\alpha_2$ wavelengths. Diffraction profile corresponding to $\text{CrK}\alpha_1$ radiation was fitted by Pearson VII function. Maxima of this function for all measured profiles served as input data for inter-planar lattice spacing's calculations. In the generalised Hooke's law, we used X-ray elastic constants $s_1 = -1.25 \text{ TPa}^{-1}$ and $\frac{1}{2}s_2 = 5.76 \text{ TPa}^{-1}$ obtained with the help of Eschelby-Kröner model [6]. Eventually, the diffraction profile corresponding to α -Fe $\{211\}$ planes parallel with the surface was characterized by FWHM (Full Width at Half Maximum) profile parameter which represents another parameter, often related to “degree of plastic deformation” [7] or “cold work”, because the diffraction profile broadening can be related to such phenomena as grain size, microscopic residual stresses or dislocation density [8] whose evolution is closely connected with plastic deformation.

Diffraction measurements were carried out on a vertical θ/θ X'Pert PRO MPD diffractometer equipped with monocapillary optics in the primary beam, i.e. the beam impinging on the analysed sample was pseudo-parallel, and point proportional detector. Positioning of the measured objects to the coveted locations was done by combining versatile positioning system with six degrees of freedom and laser triangulation for precise surface position determination with accuracy of approx. 5 μm .

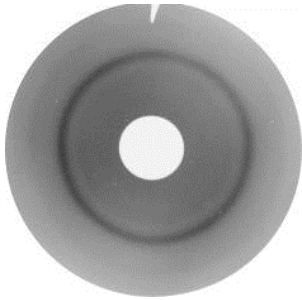
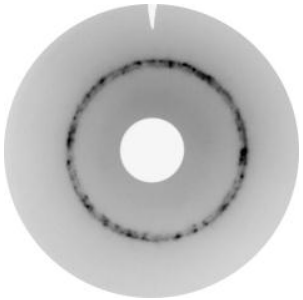
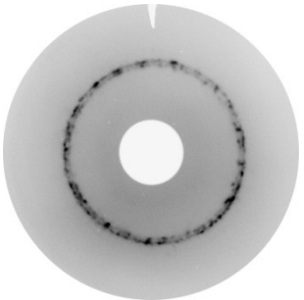
In addition to XRD analyses, hardness (HV5) was measured on the surface of both samples with 4 points on the welds, 2 points on heat-affected zone surrounding the welds from both sides and in further 8 points up to the distance of 10 mm from the welds' centre. Microstructure of the weld-heat affected zone (HAZ)-base material was observed on metallographic cross-sections.

Results

Prior to the XRD analyses of residual stresses by „ $\sin^2\psi$ “ method, diffraction patterns capturing $\{211\}$ α -Fe Debye rings were obtained. Tab. 1 shows the selection of three patterns: one from the initial state of the steel sheets prior to laser welding and one from each object 2 mm far from the welds' boundaries. The six angles of deflection for each object are summarized in Tab. 2. Metallographic cross-sections of both welds can be seen in Fig. 1. Surface distributions of macroscopic residual stresses can be seen in Figs. 2 and 3 as well as corresponding FWHM parameters in Fig. 4 and 5.

Surface distribution of hardness (HV5) did not revealed any apparent changes between the welds and their vicinity with hardness in the base material reaching approximately 180 HV, 220 HV in the HAZ and from 250 to 280 HV in the welds.

Tab. 1 Backscatter diffraction patterns with Debye rings of α -Fe $\{211\}$ planes.

Sample, area	2 m/min, 2 mm from the weld's boundary	15 m/min, 2 mm from the weld's boundary	state prior to laser welding
Diffraction pattern			

Tab. 2 Deflection of both analysed bodies in seven equidistant points in the direction perpendicular to the welds.

Point	Deflection of sample 2 m/min	Deflection of sample 15 m/min
1	-1° 4'	2° 20'
2	-1° 3'	2° 25'
3	-1° 3'	2° 25'
4	-0° 8'	2° 25'
5	-0° 7'	2° 20'
6	-0° 8'	2° 20'

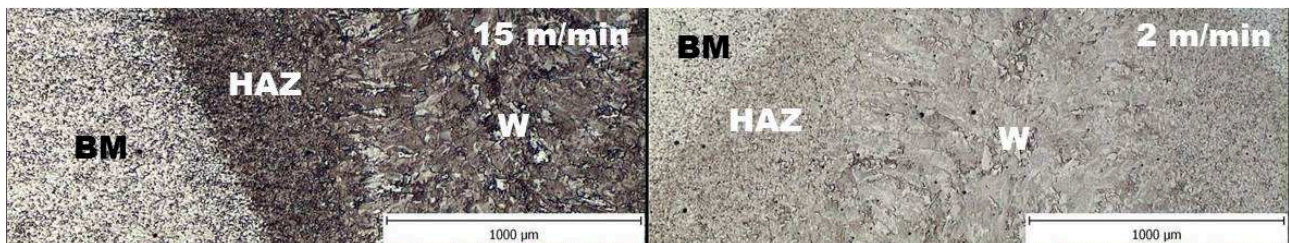


Fig. 1 Microstructure of both samples in metallographic cross-sections. BM stands for base material and W for weld.

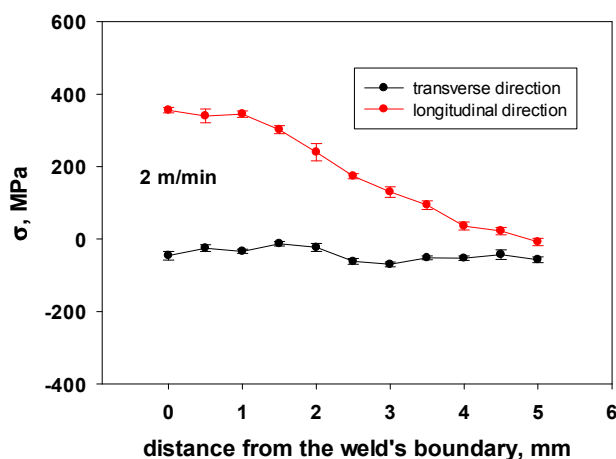


Fig. 2 Surface distribution of residual stresses in the vicinity of the laser weld created with the HPDL beam speed of 2 m/min.

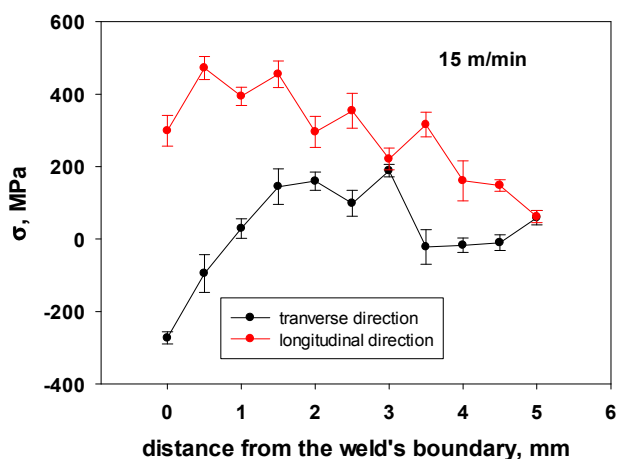


Fig. 3 Surface distribution of residual stresses in the vicinity of the laser weld created with the HPDL beam speed of 15 m/min.

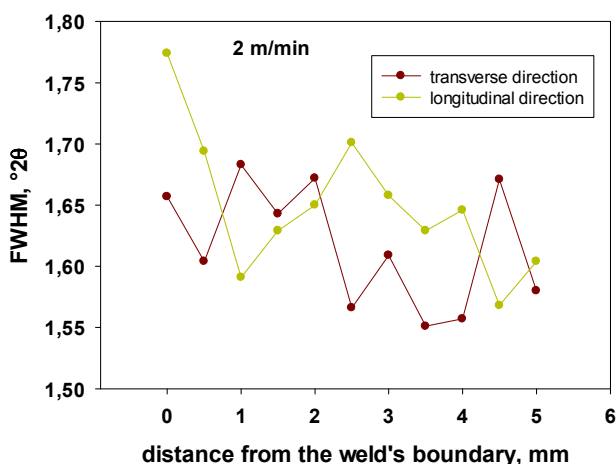


Fig. 4 Surface distribution of FWHM of α -Fe {211} diffraction profile of planes parallel with the sample surface; measured in the vicinity of the laser weld created with the HPDL beam speed of 2 m/min.

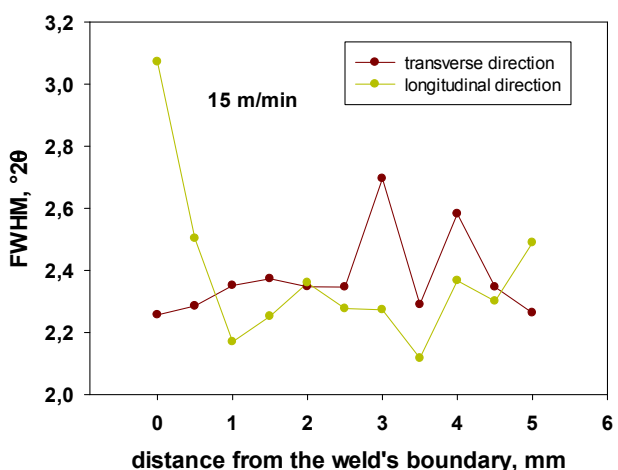


Fig. 5 Surface distribution of FWHM of α -Fe {211} diffraction profile of planes parallel with the sample surface; measured in the vicinity of the laser weld created with the HPDL beam speed of 15 m/min.

Discussion

The structure of the material in the vicinity of welds was suitable for residual stress determination by means of XRD, the irradiated surface volume did not exhibit coarse grain character which sometimes renders the choice of XRD as untrustworthy and calls for neutrons [9]. The actual welds were not analysed for residual stresses by XRD, but their microstructure seen in Fig. 1 indicates substantial grain coarsening.

From the comparison of representative Debye rings from both samples (Tab. 1) emerges the fact that the structure in the vicinity of the weld created with lower speed is distinguished by smaller grains of b.c.c. iron. It is, thus, finer-grained than the areas adjacent to the weld done with almost one order of magnitude higher speed of 15 m/min. Moreover, there is virtually no difference between Debye ring obtained from base material and the area near weld done at 15 m/min. Taking the effect of temperature-related phenomena, the performed measurements affirm that laser welding with lower beam speed leads to more pronounced heat impact of the structure. This is in agreement with a model in [10] which states that heat input is inversely proportional to laser beam speed.

On the surface of both the objects under investigation, anisotropic biaxial state of stress was established, i.e. $\sigma_T \neq \sigma_L$. Residual stresses σ_L in the direction parallel with the welds are tensile in all measured areas and decrease in value with larger distance from the welds' boundaries. The decline has monotonous character for the sample 2 m/min, but oscillations between neighbouring areas occur in the case of the body with 15 m/min weld as seen in Fig. 6.

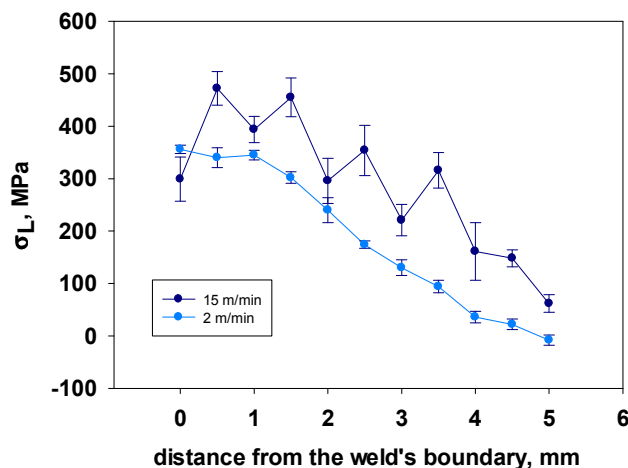


Fig. 6 Comparison of tensile residual stresses in the parallel direction with the welds.

Whereas character of σ_L surface distributions is similar, the stresses in perpendicular direction to the welds are qualitatively different for both the samples. The stresses σ_T are within comparatively narrow interval from -70 to -13 MPa for the sample 2 m/min which is in stark contrast to the other sample where the stresses rise from approx. -300 MPa to approx. 150 MPa within the 1.5 mm wide area fast beside the weld's boundary. It should be also noted that the sample joined with larger laser beam speed exhibits larger angular distortion as shown in Tab. 2.

From the comparison of all four surface distributions of $\{211\}$ α -Fe FWHM parameter, it is visible that higher values are seen for faster beam speed, see Fig. 4 versus Fig. 5. Both areas closest to the welds show apparent increase in this parameter, but only for diffraction profiles measured in longitudinal directions, i.e. parallel with the welds. The apparent difference between FWHM values in both samples even 5 mm from the boundary, i.e. approximately 1.6 and 2.2 in 2 m/min and 15 m/min, respectively, calls for further investigation of relevant real structure parameters such as microstrains and dislocation density.

Summary

Larger angular distortion of the body with a laser weld is exhibited by the sample manufactured with approximately 8 times bigger speed of HPDL beam. This sample is in the immediate vicinity characterized by substantial compressive residual stresses in the direction perpendicular to the weld. Nevertheless, the big difference in laser beam speed has no impact of hardness on the surface of the welds and their vicinity.

Acknowledgments – This research was carried out in the frame of research project TA02011004 (Technology Agency of the Czech Republic).

References

- [1] J. Lawrence, L. Li, Wettability characteristics of an $\text{Al}_2\text{O}_3/\text{SiO}_2$ -based ceramic modified with CO_2 , Nd:YAG, excimer and high-power diode lasers, *J. Phys. D* 32 (1999) 1075-1082.
- [2] G.A. Moraitis, G.N. Labeas, Residual stress and distortion calculation of laser beam welding for aluminum lap joints, *J. Mat. Proc. Tech.* 198 (2008) 260-269.
- [3] Macherauch E., Müller P.: Das $\sin^2\psi$ -Verfahren der röntgenographischen Spannungsmessung, *Zeitschrift für angewandte Physik* 13 (1961) 33 – 38.
- [4] R.A. Winholtz, J.B. Cohen, Generalised Least-squares Determination of Triaxial Stress States by X-ray Diffraction and the Associated Errors, *Aust. J. Phys.* 41 (1988) 189-199.
- [5] W.A. Rachinger, A Correction for the $\alpha_1 \alpha_2$ Doublet in the Measurement of Widths of X-ray Diffraction Lines, *J. Sci. Instrum.* 25 (1948) 254 - 259.
- [6] J.D. Eshelby, The Determination of the Elastic Field of an Ellipsoidal Inclusion, and Related Problems, *Proc. Roy. Soc. A* 241 (1957) 376 – 396.
- [7] P. S. Prev y, The measurement of subsurface residual stress and cold work distributions in nickel base alloys, *Residual Stress in Design, Process & Materials Selections*, ed. WB Young, Metals Park, OH: Am. Soc. For Metals, 1987, 11-19.
- [8] J. Pe i ka, R. Ku el, A. Dronhofer, and G. Eggeler, The evolution of dislocation density during heat treatment and creep of tempered martensite ferritic steels, *Acta materialia* 51, no. 16 (2003) 4847-4862.
- [9] Y.Tomota, P. Luk   , D. Neov, S. Harjo, Y. R. Abe, In situ neutron diffraction during tensile deformation of a ferrite-cementite steel, *Acta materialia*, 51 (2003) 805-817.
- [10] K. Y.Benyounis, A. G. Olabi, M. S. J. Hashmi, Effect of laser welding parameters on the heat input and weld-bead profile. *Journal of Materials Processing Technology* 164 (2005) 978-985.